



1 **Improved real-time bio-aerosol classification using Artificial Neural Networks**

2

3 **Maciej Leśkiewicz<sup>1</sup>, \*Miron Kaliszewski<sup>2</sup>, Maksymilian Włodarski<sup>2</sup>, Jarosław Młyńczak<sup>2</sup>, Zygmunt**  
4 **Mierczyk<sup>2</sup>, Krzysztof Kopczyński<sup>2</sup>.**

5

- 6 1. PCO S.A. ul. Jana Nowaka-Jeziorańskiego 28, 03-982 Warsaw, Poland.  
7 2. Institute of Optoelectronics, Military University of Technology, ul. Gen. Witolda Urbanowicza 2,  
8 00-908 Warsaw, Poland

9

10 \*Corresponding author: [miron.kaliszewski@wat.edu.pl](mailto:miron.kaliszewski@wat.edu.pl)

11

12

13 **Keywords: Bio-aerosol, Fluorescence, Real-time analysis, Artificial Neural Network, PBAP.**

14

15 **1. Abstract**

16 Air contamination has had stronger and stronger impact on everyday life of humans. An  
17 increasing number of people are aware of the health problems that may result from inhaling air  
18 containing dust, bacteria, pollens or fungi. Society is awaiting anxiously for a system that could  
19 inform them in real-time about a real danger that is suspended in the air. The devices, currently  
20 available on the market, are able to detect some particles in the air, but cannot classify them by the  
21 health threats. Fortunately, a new type of technology is emerging as a really promising solution.  
22 Laser based bio-detectors are opening a new era in aerosol research. They are capable of  
23 characterizing a great number of individual particles in seconds by analyzing optical scattering and  
24 fluorescence characteristics. In this study we demonstrate application of Artificial Neural Network  
25 (ANN) to real-time analysis of single particle fluorescence fingerprints. We gathered a total of 114779  
26 spectra of 48 aerosols. We discuss an entirely new approach to data analysis using decision tree  
27 comprising 22 independent neural networks. Applying confusion matrices and ROC analysis the best  
28 sets of ANN's for each group of similar aerosols has been determined. As a result we achieved very  
29 high performance of aerosol classification in real-time. We found that for some substances that have  
30 characteristic spectra almost each particle can be properly classified. The aerosols with similar  
31 spectral characteristics can be classified as a specific cloud with high probability.

32

33 **2. Introduction**

34 The ambient air contains a variety of particles like dust, bacteria, pollens, fungi and other parts of  
35 biological and non-biological origin (Pöhlker et al., 2013) (Górný, 2004). The aerosols are involved in  
36 various atmospheric processes like ice nuclei formation, precipitation and global climate effects  
37 (Deguillaume et al., 2008) (Fröhlich-Nowoisky et al., 2016) (Gabey et al., 2010) (Pósfai and Buseck,  
38 2010) (Fuzzi et al., 2015). They also strongly influence human health (Davidson et al., 2005) (Pope III  
39 and Dockery, 2006) (Michaels, 2017) (Shiraiwa et al., 2012). Therefore, the characterization of  
40 ambient air is important for estimating potential health hazards and environmental impact  
41 (Mauderly and Chow, 2008) (Lim et al., 2005). Standard methods of aerosol composition assessment  
42 usually include microscopic inspection or molecular analysis of filter (Miaskiewicz-Peska and  
43 Lebkowska, 2012), tape or liquid trapped particles. Nevertheless, they suffer from low time  
44 resolution due to periodical and relatively long analytical procedures. They are also ineffective for the  
45 detection of non-culturable microorganisms (Blais-Lecours et al., 2015) (Trafny et al., 2014).

46 The detection and classification of biological particles is possible using fluorescence techniques



47 due to the presence of proteins, NADH, and some vitamins that emit light when excited with UV light  
48 (Lakowicz, 1999). This feature is utilized in single particle fluorescence detectors. In the flowing air  
49 each particle is characterized for size/shape using light scattering as well as fluorescence properties.  
50 This approach ensures continuous measurement and immediate response. Thus the analysis process  
51 can be facilitated and accelerated compared with other commonly used analytical procedures (Hill et  
52 al., 1999) (Choi et al., 2014) (Taketani et al., 2013) (Feugnet et al., 2008).

53 Several studies using single particle fluorescence detectors demonstrated that fluctuations of  
54 aerosol concentration and variations in its fluorescence properties are strongly dependent on the  
55 season, day time, location and a place occupancy (Gabey et al., 2011) (Huffman et al., 2010) (Pinnick  
56 et al., 2004) (Bhangar et al., 2014) (Fennelly et al., 2018). Each single particle passing the instrument  
57 is labelled with the time, scattering properties (size and/or shape) and fluorescence characteristics. It  
58 is obvious that continuous single particle measurements bring a new potential and quality to  
59 environmental research. However, particles of the same type and batch display slightly different  
60 spectral characteristics due to variations in biochemical composition, size, age in a population  
61 (Agranovski et al., 2003), degradation or stress level (Lee et al., 2010) and the particle position within  
62 instrument's interrogation point (Pan et al., 2011). The simple statistics, like data averaging and  
63 graphical spectra representation, are not sufficient. Therefore, the huge amount of data and  
64 occurring spectral variations require more advanced algorithms supporting automatic data  
65 classification. Various analytical methods of particle discrimination and classification were applied. It  
66 has been shown that Principal Component Analysis (PCA), Linear Discriminant Analysis (LDA),  
67 Hierarchical cluster Analysis (HCA) of fluorescence spectra strongly increases discrimination of  
68 particles compared with methods based on spectra averaging or fluorescence threshold (Leśkiewicz  
69 et al., 2016) (Kaliszewski et al., 2013) (Pan et al., 2012) (Hernandez et al., 2016). Artificial neural  
70 network (ANN) is an emerging analytical approach that becomes more widely and successfully  
71 applied in various life domains like chemical analysis (Borecki et al., 2008), image recognition  
72 (Antowiak and Chałasińska-Macukow, 2003), data mining and weather forecasting (Purnomo et al.,  
73 2017). It has been shown that ANN can be applied in bio-aerosol classification (Kohlus and Bottlinger,  
74 1993). However, it usually requires more user input comparing to other analytical procedures (Ruske  
75 et al., 2017).

76 This paper focuses on the application of ANN for real time discrimination of bio-aerosols basing  
77 on single particle fluorescence characteristics. We demonstrated a new approach to data analysis  
78 using ANN allowing automatization of data preparation procedures and minimum user involvement.

79

### 80 3. Materials and methods

#### 81 3.1. Experiment

##### 82 3.1.1. BioAeRosol Detector (BARDet)

83 The detailed information concerning construction and parameters of the instrument used for  
84 the experiments was presented in our previous work (Kaliszewski et al., 2016). In general, the  
85 ambient air is continuously drawn through the nozzle. It is focused with sheath flow of filtered air.  
86 Particles in the focused air pass through the BARDet's chamber where they are interrogated by a  
87 16mW CW laser beam generated by a diode laser operating at 375 nm wavelength (CUBE, Coherent).  
88 The backward and forward scattered signals are detected with two PMT's (H6780, Hamamatsu)  
89 mounted at the 35° and 145° angle to the laser beam axis.

90 The fluorescence of particles is measured at a 90° angle to the laser beam with 32 channel PMT  
91 (A10766, Hamamatsu). The longpass filter with cutting edge at 400 nm (Edmund Optics) separates



92 the fluorescence signal from scattered light. The multichannel PMT measures fluorescence in 18  
 93 active channels in the range of 415.4-643.5 nm. The channels are grouped in 7 bands. The remaining  
 94 channels are not used. The band configuration is presented in Table 1.

95

96 Table 1. Configuration of bands in the multichannel PMT.

97

BARDet's Fluorescence Bands	Bandwidth [nm]
B1	415.4 – 429.3
B2	443.1 – 456.8
B3	470.5 – 484.2
B4	497.8 – 524.9
B5	538.3 – 565.0
B6	578.3 – 604.6
B7	617.6 – 643.5

98

### 99 3.1.2. Biological Aerosols

100 For the tests, dry powders of harmless substances were used, since they did not need a  
 101 specialized aerosol protection chamber. The samples used for this study are listed in Table 2. To  
 102 perform numerous experiments, disposable vials were used, one for each aerosol sample. It  
 103 prevented cross contamination between measured samples. The aerosols were generated from  
 104 modified 50 ml Falcon tubes placed on the vortex. The vials in the lower part contained two  
 105 connectors for silicon tubes. Vortexed particles were entrained and formed an aerosol cloud inside  
 106 the Falcon tube. The aerosolized particles were aspirated from the vial to BARDet's aerosol inlet.  
 107 Each tube contained about 50 mg of the dry powder sample. During aerosol generation filtered air  
 108 was supplied into the vial to compensate the BARDet's flow. The concentration of the aerosols was  
 109 adjusted with vibration frequency of vortex. The measurement started after the aerosol reached  
 110 homogeneous concentration. The experimental setup is shown in figure 1.

111

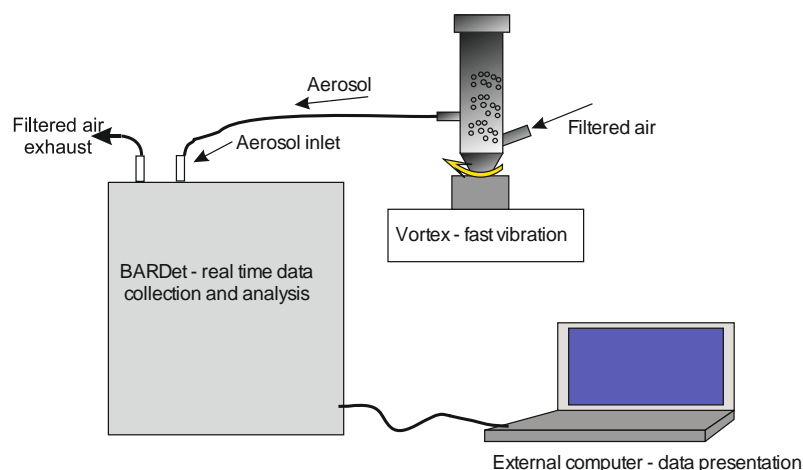
112 Table 2. List of all substances used in experiment.

113

	Abbreviation	Name	Source	Group
1	FM7	Fluoromax microspheres 7 um	Thermo scientific	standard 1
2	Rib	Riboflavin	Sigma-Aldrich	standard 2
3	BGP	Bermuda grass pollen	Duke Sci. Corp.	pollen
4	CP	Corn pollen	Duke Sci. Corp.	
5	CA	<i>Corylus avellana</i> pollen	Own collectionon	
6	LP	<i>Lycopodium</i> pollen	Fluka	
7	PPP	<i>Poa pratensis</i> pollen	Sigma-Aldrich	
8	RP	Ragweed pollen	Duke Sci. Corp.	
9	SCP	<i>Secale cereale</i> pollen	Sigma-Aldrich	



10	SP	Spruce pollen	Own collection	
11	AA	<i>Abies alba</i> pollen	Own collection	
12	UDP	<i>Urtica dioica</i> pollen	Own collection	
13	PSP	<i>Pinus sylvestris</i> pollen	Own collection	
14	PNP	<i>Pinus nigra</i> pollen	Own collection	
15	LPP	<i>Lycopodium</i> pollen (Poland)	Own collection	
16	PMP	Paper mulberry pollen	Duke Sci. Corp.	
17	ATP	<i>Artemisia tridentata</i> pollen	Sigma-Aldrich	
18	AAP	<i>Artemisia absinthium</i> pollen	Sigma-Aldrich	
19	CPP	<i>Chenopodium</i> pollen	Own collection	
20	BWF	Buck wheat flour	Regular shop	flour
21	PF	Potato flour	Regular shop	
22	RF	Rice flour	Regular shop	
23	TF	Tapioca flour	Regular shop	
24	WF	Wheat flour	Regular shop	
25	Trp	Tryptophan	Sigma-Aldrich	amino acids and proteins
26	Phe	Phenylalanine	Sigma-Aldrich	
27	BSA	Bovine Serum Albumin	POCH Poland	
28	OVA	Ovalbumin	POCH Poland	
29	Ambio	<i>Bif. animalis</i> , <i>S. boulardii</i> , <i>S. thermophilus</i> , <i>L. casei</i> , <i>L. bulgaricus</i>	Pharmacy	bacteria in medium
30	LCB	<i>Lactobacillus bulgaricus</i>	Pharmacy	
31	LF	<i>Bifidobacterium animalis</i> , <i>L. acidophilus</i>	Pharmacy	
32	BA	Bacteriological Agar	Sigma-Aldrich	medium
33	BAB	Blood Agar Base	Sigma-Aldrich	
34	LB	Luria broth	Sigma-Aldrich	
35	NB	Nutrient broth	Sigma-Aldrich	
36	BTSTG	<i>Bacillus thuringiensis</i> spores technical grade	Agricultural	Bacterial spore with admixtures
37	SB	<i>Saccharomyces boulardii</i>	Pharmacy	fungi with admixtures
38	SC	<i>Saccharomyces cerevisiae</i>	Regular shop	
39	LS	<i>Lycoperdon</i> spores	Own collection	fungal spores
40	JGSS	Johnsons grass smut spores	Duke Sci. Corp.	smut spore (fungal spore)
41	BGSS	Bermuda grass smut spores	Duke Sci. Corp.	
42	ACFTD	AC Fine Test Dust	Duke Sci. Corp.	other
43	NT	Nivea talc	Regular shop	
44	PPD	Printer paper dust	Regular shop	
45	PTD	Paper towel dust	Regular shop	
46	Cin	Cinnamon	Regular shop	
47	Cel	Celulose	Sigma-Aldrich	
48	GGL	Grinded Green Leaves	Own collection	



115  
116 Figure 1. Setup of aerosol generation, data recording and analysis.  
117

### 118 3.1.3. Data acquisition method and pre-processing

119 The fluorescence of each particle was recorded in 7 bands. It creates a time series of the signals  
120 which has to be pre-processed before further analysis. There are two steps of gathering data. First  
121 one is performed by internal BARDet's software, which is responsible for controlling the instrument  
122 and the acquisition of raw signals. Then data is forwarded to a pre-processing module of analysis  
123 software. Its first task is to extract valuable signals from the noise (three sigma rule). Then a  
124 normalization procedure is required. It is realized first by subtracting the average value of signal and  
125 then it normalizing to its standard deviation. The main goal was to analyze shape of emission  
126 spectrum (not signal strength).

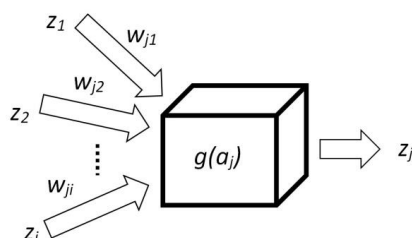
127 An Important aspect of the data acquisition process was monitoring the rate of generation of  
128 aerosol, which should be stable (not too high or spontaneous). Finally, we gathered a total of 114 779  
129 spectral characteristics of 48 aerosols which gives in average almost 2400 fluorescence signals per  
130 substance. It is important to note that fact because of its statistical value for the further analysis.

## 131 3.2. Data analysis

### 132 3.2.1. ANN (Artificial Neural Network)

#### 133 3.2.1.1. Basics

134  
135  
136 There are many types of Artificial Neural Networks (ANN), but in this paper only the  
137 backpropagation algorithm is demonstrated because it is one of the most practical. The main concept  
138 of this algorithm is based on a model of neuron that has two tasks. It aggregates signals (1) and then  
139 processes them by an activation function (2), which, in this research, is a sigmoid. The result of such  
140 single processing is a new signal  $z_j$  propagated to other neurons (Figure 2).



141  
 142 Figure 2. Mathematical model of single neuron cell.  
 143

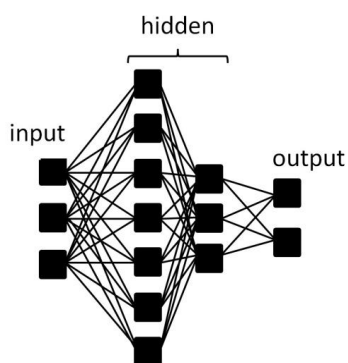
$$a_j = \sum_i w_{ji} z_i \quad (1)$$

144  
 145  $a_j$ - aggregated signal,  $w_{ji}$ - weight that connects neuron  $i$  with  $j$ ,  $z_i$ - signal (input).

$$g(a_j) = \frac{1}{1 + e^{-\beta a_j}} \quad (2)$$

147  
 148  $g(a_j)$  – sigmoidal function,  $\beta$ - parameter (steepness) of sigmoid curve.

149  
 150 The structure of neural network is formed by layers of neurons: input, hidden and output. In this  
 151 research input neurons are fluorescence spectrum and output neurons represent substances. In  
 152 hidden layers (one and two hidden layers were examined) mostly actual computations are done. The  
 153 schematic representation of neuron layers is presented in Figure 3.



154  
 155 Figure 3. Typical topology of artificial neural network.  
 156

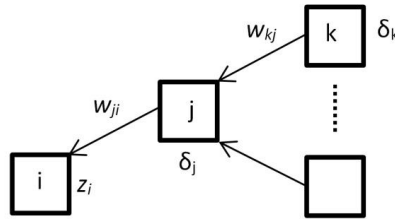
157 The described algorithm is the supervised learning method that requires training data for a  
 158 teaching process. This allows one to calculate an error between the showed target and the ANN  
 159 response. Every problem is related to minimizing output error which is calculated as Mean Squared  
 160 Error (3).



$$E = \frac{1}{2} \sum_{k=1}^c (y_k - t_k)^2 \quad (3)$$

161  $E$  – Mean Squared Error,  $t_k$ - observed value (target),  $y_k$ - calculated response,  $k$ -output neuron,  $c$  –  
 162 number of output neurons.

163 Gradient descent method is used to find a minimum of error function. Error is dependent on  
 164 network weights  $\Delta w_{ji}$  which might be adjusted (4). In order to update weights correctly, the first one  
 165 needs to propagate error backward by calculating partial derivatives  $\delta_j$  (5) (Figure 4). All  
 166 mathematical details are well described by Ch. M. Bishop book (Bishop, 1995).



167

168 Figure 4. Model of backward error propagation.

$$\Delta w_{ji}(t) = -\eta \delta_j z_i + m \Delta w_{ji}(t-1) \quad (4)$$

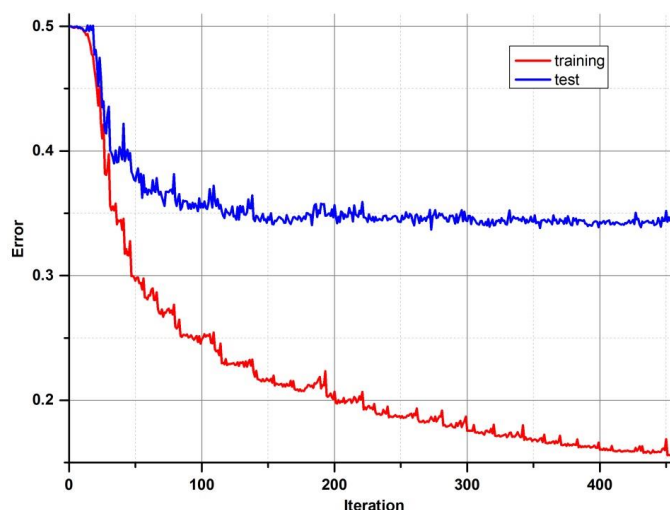
169  $\eta$ - learning rate,  $m$  - momentum,  $t$  - iteration.

170

$$\frac{\delta E}{\delta w_{ji}} = \frac{\delta E}{\delta a_j} \frac{\delta a_j}{\delta w_{ji}} = \delta_j z_i \quad \delta_j = g'(a_j) \sum_k w_{kj} \delta_k \quad (5)$$

171 The learning rate factor determines the size of the steps while momentum parameter helps to  
 172 skip local minimum by adding a fraction of the weight correction from the last step.

173 After the correction of all weights of ANN, the output error is examined and the procedure  
 174 starts again unless an error level is low enough and there is no overfitting. All data are divided into  
 175 three different sets: training, test and validation. For calculations during the learning process, only  
 176 the first two are used. In order to determine whether it is time to stop teaching, one has to observe  
 177 an error in the test set. There will be a moment when this error comes to be constant or starts  
 178 increasing due to the overfitting of training data (Figure 5). The validation data set may be useful for  
 179 confronting different models or just to verify the current model on completely separate set of data.



180

181 Figure 5. Example of error minimizing during training process.

### 182 3.2.1.2. Implementation of ANN for BARDet

183 There are statistical commercial software packages available that provide ANN modules as one  
184 of the methods to analyze the data. It is worthwhile noting that customized software was developed  
185 for the purpose of this research. This approach helped to understand ANN in depth and let to the  
186 development of software that is not only responsible for data pre-processing and network training,  
187 but also (mainly) for solving a real time classification problem.

188 Ruske et al. in their studies (Ruske et al., 2017) compared various algorithms to analyze single  
189 particle data and noted that ANN requires much more user input. However, we present the method  
190 to overcome this inconvenience by automatizing the process and implementing procedures that  
191 simplifies and improve analysis.

192 The main disadvantage of ANN is the fact that it is a parametrized algorithm. How well it works  
193 depends strictly on a proper choice of the best possible factors, which may be different for each  
194 problem. There are two types of factors that influence the ANN outcome. The first one corresponds  
195 to the architecture of ANN which comprises: number of layers, neurons and activation function  
196 parameter. The second one determines the learning process: momentum and learning rate. The last  
197 one can be tuned during the learning process to make it much faster. The “bold driver” procedure  
198 was chosen for that purpose. It continuously increases the learning rate unless an error is higher  
199 from that before the change. If it is, the algorithm radically decreases the learning rate and obtains  
200 weights from the last step again. Teaching ANN is a stochastic process caused by using randomly  
201 chosen initial weights. It was found that the best procedure for this investigation would be to make  
202 all optimization processes that way. Therefore, parameters of ANN, responsible both for structure  
203 and learning process, are randomly selected until the desired result is reached. In fact, the  
204 calculations are done automatically and simultaneously for several models due to multi core oriented  
205 software. The benefits of this approach are: time saving and high effectiveness of finding the best  
206 model. The last one is especially important, because the goal is to create a model that produces the  
207 best results, which doesn't necessary mean creating a more complicated network (more neurons or





208 layers).

209 **3.2.2. Model evaluation**

210 The main goal of analysis described in this paper is to find a solution to the bio-aerosol  
 211 classification problem. When a training process ends, a final model is created: a network, which has a  
 212 unique structure and a set of weights. One can create many of them and make a comparison only by  
 213 a final error. It is not the best solution, because the goal is to distinguish patterns in data  
 214 consistently, not to produce a network with a minimal error. That is why there is a need to make a  
 215 final analysis of the results and evaluate the model in accordance with the best classification  
 216 performance.

217 The standard method for visualization of results is a confusion matrix which will be necessary for  
 218 Receiver Operating Characteristics (ROC) analysis (Fawcett, 2006). It simply shows what fraction of  
 219 population for each class is predicted correctly or not. Each element from the data set increments  
 220 one of the fields: TP, TN, FN and FP (Table 3). If it belongs to a diagonal (TP, TN), it was classified  
 221 correctly.

222

223 Table 3. Structure of confusion matrix.

224

		Predicted class	
		positive	negative
True class	positive	True Positives (TP)	False Negatives (FN)
	negative	False Positives (FP)	True Negatives (TN)

225

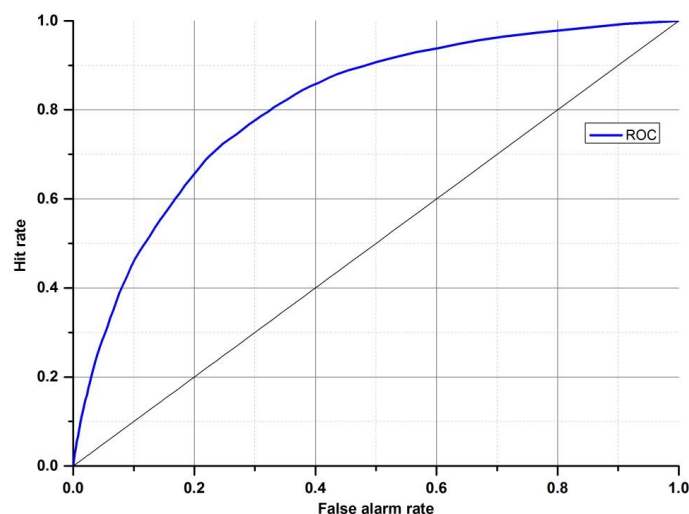
226 The ROC graphs are very simple but useful tools for discovering whether a classifier is worth  
 227 using or if it makes a random classification. It is based on two rates from confusion matrix: hit rate (6)  
 228 and false alarm rate (7).

$$\text{hit rate (true positive rate)} = \frac{TP}{TP + FN} \quad (6)$$

229

$$\text{false alarm rate (false positive rate)} = \frac{FP}{FP + TN} \quad (7)$$

230 Each discrete classifier has a threshold level that assigns an element to a positive or negative  
 231 class. The points of ROC graph (Figure 6) represent the classifier for many thresholds. The most  
 232 desired curve reaches the highest true positive rate with the lowest false positive rate (convex line).  
 233 The random classifier, in turn, has a hit rate equal to a false alarm rate despite threshold variation  
 234 (diagonal line). To identify ROC analysis with one coefficient, the area under the curve (AUC) may be  
 235 used. The higher value of AUC results in better performance (0.5-means random, 1-excellent).



236

237 Figure 6. ROC graph with an example of classifier (blue).

238 The confusion matrix and ROC analysis described above were defined for two class problems  
239 (positive, negative). There is a straightforward way to expand it for the multi-class problem. One  
240 needs to take a desired class versus all other classes. Then there is a possibility to compare how good  
241 the classifier for specific classes within one model is.

## 242 4. Results

### 243 4.1. ANN performance

244 First attempts were made to distinguish all substances using only one neural network model. The  
245 tests revealed that it is impossible due to the huge number of samples (48 aerosols) and only a few of  
246 them presented significantly different fluorescence spectra. A more practical approach to this  
247 problem would be to create several groups (considering information about aerosols), but we did not  
248 want to make any classes *a priori*. Although the demonstrated ANN type needs a training, which  
249 requires a set of known classes, further tests showed that there is a possibility to find similarities  
250 between substances through the analysis of confusion matrices. It was achieved after many trials of  
251 matching substances, which were not well separated, into new groups and checking if they are good  
252 enough on ROC graphs. Consequently, this procedure was also applied to those new groups.

253

254 All examples demonstrated below were calculated on the test data sets, not training data. In the  
255 first presented network (Figure 7), which try to classify all of 48 substances (group 0), four aerosols  
256 reached very high accuracy of separation ( $AUC > 0,9$ ). The best separation was achieved for  
257 fluorescent microspheres (FM7). In this case 98.5% of all FM7 particles were correctly classified. Very  
258 high separation efficiency was achieved for riboflavin (Rib), NT (Talc) and LCB (*Lactobacillus*  
259 *bulgaricus*). The remaining aerosols were divided into 3 separate groups that gather the most similar  
260 substances (group 1-3) (Table 4). The subsequent groups up to 21 represent individual ANNs leading  
261 to the final classification of the aerosol.

262

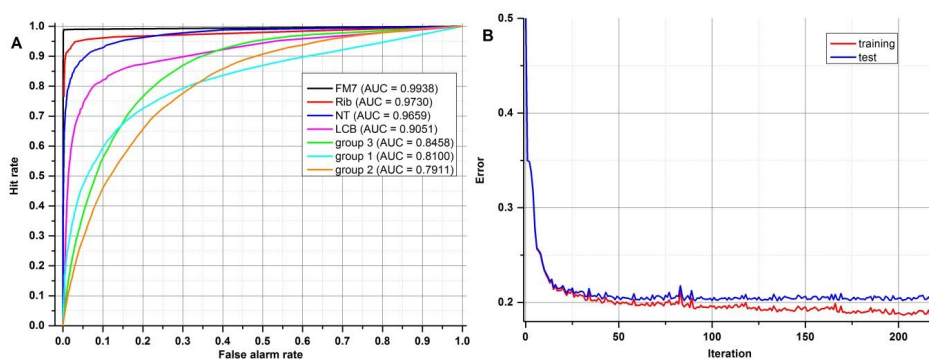
263

264



265 Table 4. Confusion matrix of all aerosols.  
 266

		predicted						
		FM7	Rib	NT	LCB	group 3	group 1	group 2
true	FM7	98.5	0	0	0.3	0.1	0	1.1
	Rib	0.1	91	0.5	3.1	1.2	0.6	3.4
	NT	0	0.1	86.5	0	9.3	0.3	3.8
	LCB	1	1.6	0.6	72.7	3.9	10.7	9.5
	group 3	0	0.7	6.6	0.6	63.3	12	16.8
	group 1	0.2	1	1	7.9	12.5	61.6	15.8
	group 2	0.1	1.2	3.8	6.6	17.6	13.2	57.4



267

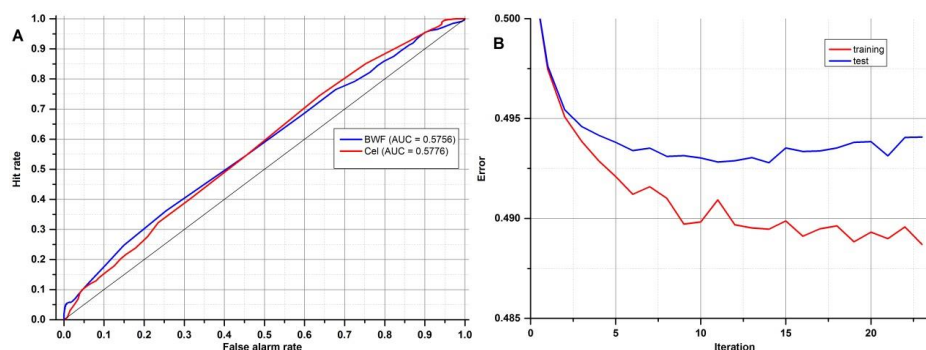
268 Figure 7. (A) ROC and (B) error progress of ANN that classifies all samples.

269 Table 5 and Figure 8 show results achieved for two substances that have very similar spectrum  
 270 and calculated AUCs are not much higher than in a random classifier. This example clearly shows why  
 271 we are not always able to classify each particle of aerosol with 100% accuracy. However, just a  
 272 representative number of measured particles allows the proper prediction of aerosol types within a  
 273 few seconds. This is easy to observe during real time detection, because counts allocated in  
 274 confusion matrix tend to reach a stable state quite quickly.

275

276 Table 5. Confusion matrix of two substances that have very similar spectra.

		predicted	
		BWF	Cel
true	BWF	54.8	45.2
	Cel	45.6	54.4



277

278 Figure 8. ROC (A) and error progress (B) of ANN that classifies two very similar samples.

279

280

#### 4.2. Classification tree

281

282

283

284

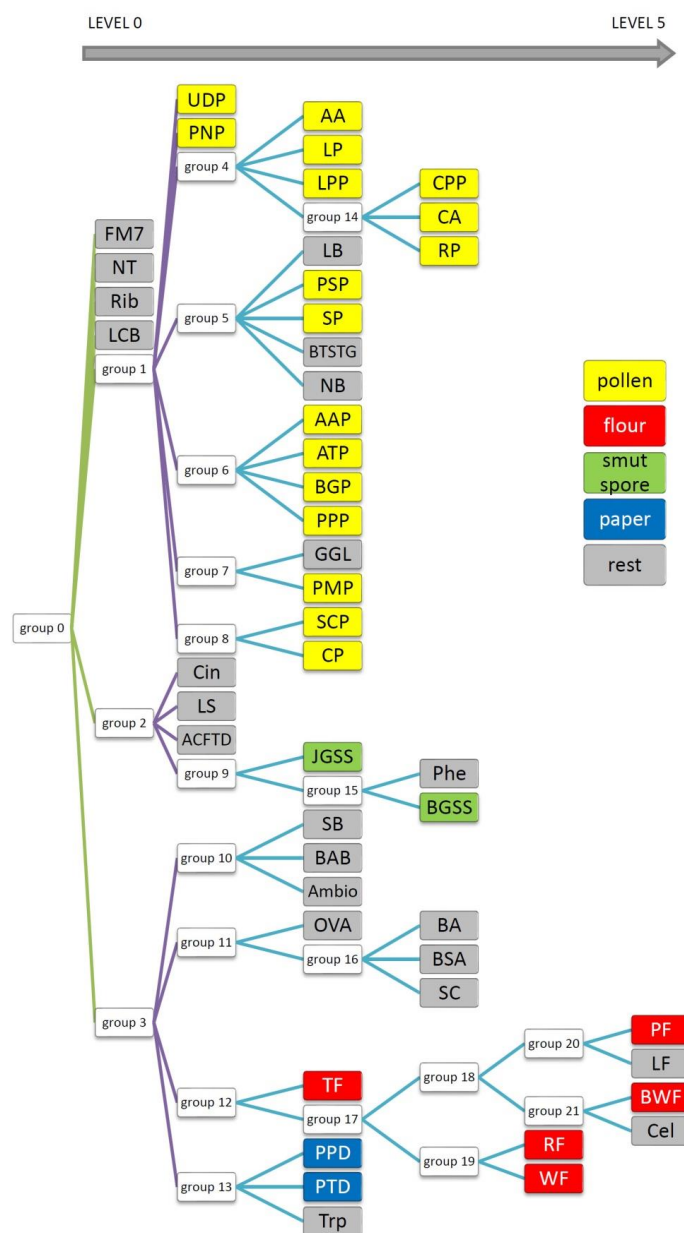
285

286

287

288

Finally, to achieve the best possible classification, the decision tree was created (Figure 9). It comprises not one but 22 models. It is difficult to present confusion matrices and ROC graphs for all neural networks in this paper, so only the most interesting one has been discussed. Here, each node represents a network that classifies a group of aerosols. The aerosols on the left side of the diagram show the most distinct differences, thus they are easy to classify (Level 0). In the right direction (Level 1-5) this task is much more demanding due to similar spectrum and the separation is less probable in accordance to single particles, although still it is very useful from a practical point of view for aerosol cloud discrimination.



289

290 Figure 9. Decision tree consists of 22 ANN separating 48 substances.

291 At first glance one could see that FM7 and Rib are very well recognized, but that was expected,  
 292 because these are standards of fluorescence. Surprisingly, NT and LCB aerosols were also separated  
 293 from the others (Level 0 network). Further analysis of the tree structure identifies a correlation  
 294 between samples and their real categories, especially it is noticeable for Pollens, which are allocated  
 295 on a separate branch of that tree and all stems from group 1. Most of them were classified on the  
 296 third level. Interestingly all grass pollens (AAP, ATP, BGP, PPP) belong to the same group 6. Similarly



297 both *Lycopodium* pollens from different regions of the world show close correlation, however *Abies*  
298 *alba*, which is a tree, was classified to the same group. Flowers, Smut Spores and Papers are dispersed  
299 between different levels but particular groups belong to the same branch of the tree. However, some  
300 of samples, are scattered on the whole tree area and do not correspond to any group.

301 It should be noted that the result is a system of 22 ANNs that works simultaneously. In  
302 comparison to the training process, which is rather time consuming and has to be empirically  
303 optimized, this cluster of learned ANN's delivers very high performance. Input data is processed by a  
304 single ANN in milliseconds. This performance makes neural network a great tool as a splitting node in  
305 the classification tree. Comparing to our previous results, where Principal Component Analysis was  
306 applied to analyze data from BARDet (Kaliszewski et al., 2016), the ANN allowed much better  
307 discrimination between various bio-aerosols.

## 308 5. Summary

309 In this paper the possibility of an application of the Artificial Neural Network (ANN) for a real  
310 time classification of biological aerosols was investigated. The spectral characteristics of bio-aerosols  
311 were collected using the BARDet instrument. Finally, the database consisted a large data set of 114  
312 799 samples (particle characteristics) of 48 substances. It ensured that application of the ANN was  
313 fully justified. Finally, we trained 22 neural networks and combined them into a decision tree, which  
314 was laborious and time consuming. However, trained ANN's characterized single particles in real  
315 time. Tests revealed that only several substances have such characteristic fluorescence spectra that  
316 allows correct classification of almost each particle. However, in all other cases the system was able  
317 to recognize a particular aerosol cloud. Further approximation was based on decision tree analysis  
318 where each node corresponded to a separate learned ANN. The best sets of ANN's for each group of  
319 similar aerosols were discovered utilizing confusion matrices and ROC analysis. Our intentions were  
320 to make a complete system which detects and classifies substances without creating groups *a priori*.  
321 This attitude helped to create a powerful analytical tool that works automatically and the results of  
322 classification are immediately available on the operator's screen.

323 This study proved that it is possible to create a tool for a highly effective analysis of bio-aerosols  
324 using multiple ANNs combined into decision tree. Our approach allowed automation and speed up of  
325 analysis, which reduced time and the amount of needed computing power. In a future study we will  
326 extend the database to obtain possibly vast variety of samples including bacteria and fungi. Finally,  
327 the actual performance of the system will be determined under real environmental conditions.

328

## 329 Acknowledgments

330 Presented work was supported by grant from The National Centre of Research and Development  
331 (Poland), project: "Mobile laboratory for environmental sampling and identification of biological  
332 threats" (O ROB 0031 01/ID/31/1).

333

334

## 335 Bibliography

336 Agranovski, V., Ristovski, Z., Hargreaves, M., Blackall, P. J. and Morawska, L.: Performance  
337 evaluation of the UVAPS: Influence of physiological age of airborne bacteria and bacterial  
338 stress, *J. Aerosol Sci.*, 34(12), 1711–1727, doi:10.1016/S0021-8502(03)00191-5, 2003.



- 339 Antowiak, M. and Chałasińska-Macukow, K. C. H. a: Fingerprint identification by using  
340 artificial neural network with optical wavelet preprocessing, , 11(4), 327–337, 2003.
- 341 Bhangar, S., Huffman, J. A. and Nazaroff, W. W.: Size-resolved fluorescent biological aerosol  
342 particle concentrations and occupant emissions in a university classroom, *Indoor Air*, 24(6),  
343 604–617, doi:10.1111/ina.12111, 2014.
- 344 Bishop, C. M.: *Neural Networks for Pattern Recognition*, Oxford University Press, Inc., New  
345 York, NY, USA., 1995.
- 346 Blais-Lecours, P., Perrott, P. and Duchaine, C.: Non-culturable bioaerosols in indoor settings:  
347 Impact on health and molecular approaches for detection, *Atmos. Environ.*, 110, 45–53,  
348 doi:10.1016/j.atmosenv.2015.03.039, 2015.
- 349 Borecki, M., Korwin-Pawlowski, M. L. and Beblowska, M.: A Method of Examination of  
350 Liquids by Neural Network Analysis of Reflectometric and Transmission Time Domain Data  
351 From Optical Capillaries and Fibers, *IEEE Sens. J.*, 8(7), 1208–1214,  
352 doi:10.1109/JSEN.2008.926182, 2008.
- 353 Choi, K., Ha, Y., Lee, H. K. and Lee, J.: Development of a biological aerosol detector using  
354 laser-induced fluorescence and a particle collection system, *Instrum. Sci. Technol.*, 42(2),  
355 200–214, doi:10.1080/10739149.2013.855639, 2014.
- 356 Davidson, C. I., Phalen, R. F. and Solomon, P. A.: Airborne particulate matter and human  
357 health: A review, *Aerosol Sci. Technol.*, 39(8), 737–749, doi:10.1080/02786820500191348,  
358 2005.
- 359 Deguillaume, L., Leriche, M., Amato, P., Ariya, P. a., Delort, A. M., Pöschl, U., Chaumerliac, N.,  
360 Bauer, H., Flossmann, a. I. and Morris, C. E.: Microbiology and atmospheric processes:  
361 chemical interactions of Primary Biological Aerosols, *Biogeosciences Discuss.*, 5(1), 841–870,  
362 doi:10.5194/bgd-5-841-2008, 2008.
- 363 Fawcett, T.: An introduction to ROC analysis, *Pattern Recognit. Lett.*, 27(8), 861–874,  
364 doi:<https://doi.org/10.1016/j.patrec.2005.10.010>, 2006.
- 365 Fennelly, M. J., Sewell, G., Prentice, M. B., O’Connor, D. J. and Sodeau, J. R.: Review: The Use  
366 of Real-Time Fluorescence Instrumentation to Monitor Ambient Primary Biological Aerosol  
367 Particles (PBAP), *Atmosphere (Basel)*, 9(1), 2018.
- 368 Feugnet, G., Lallier, E., Grisard, A., McIntosh, L., Hellström, J. E., Jelger, P., Laurell, F., Albano,  
369 C., Kaliszewski, M., Wlodarski, M., Mlynczak, J., Kwasny, M., Zawadzki, Z., Mierczyk, Z.,



- 370 Kopczynski, K., Rostedt, A., Putkiranta, M., Marjamäki, M., Keskinen, J., Enroth, J., Janka, K.,  
371 Reinivaara, R., Holma, L., Humppi, T., Battistelli, E., Iliakis, E. and Gerolimos, G.: Improved  
372 laser-induced fluorescence method for bio-attack early warning detection system, in  
373 Proceedings of SPIE - The International Society for Optical Engineering, vol. 7116, Thales  
374 Research and Technology, France., 2008.
- 375 Fröhlich-Nowoisky, J., Kampf, C. J., Weber, B., Huffman, J. A., Pöhlker, C., Andreae, M. O.,  
376 Lang-Yona, N., Burrows, S. M., Gunthe, S. S., Elbert, W., Su, H., Hoor, P., Thines, E.,  
377 Hoffmann, T., Després, V. R. and Pöschl, U.: Bioaerosols in the Earth system: Climate, health,  
378 and ecosystem interactions, *Atmos. Res.*, 182, 346–376,  
379 doi:10.1016/j.atmosres.2016.07.018, 2016.
- 380 Fuzzi, S., Baltensperger, U., Carslaw, K., Decesari, S., Denier Van Der Gon, H., Facchini, M. C.,  
381 Fowler, D., Koren, I., Langford, B., Lohmann, U., Nemitz, E., Pandis, S., Riipinen, I., Rudich, Y.,  
382 Schaap, M., Slowik, J. G., Spracklen, D. V., Vignati, E., Wild, M., Williams, M. and Gilardoni, S.:  
383 Particulate matter, air quality and climate: Lessons learned and future needs, *Atmos. Chem.*  
384 *Phys.*, 15(14), 8217–8299, doi:10.5194/acp-15-8217-2015, 2015.
- 385 Gabey, A. M., Gallagher, M. W., Whitehead, J., Dorsey, J. R., Kaye, P. H. and Stanley, W. R.:  
386 Measurements and comparison of primary biological aerosol above and below a tropical  
387 forest canopy using a dual channel fluorescence spectrometer, *Atmos. Chem. Phys.*, 10(10),  
388 4453–4466, doi:10.5194/acp-10-4453-2010, 2010.
- 389 Gabey, A. M., Stanley, W. R., Gallagher, M. W. and Kaye, P. H.: The fluorescence properties  
390 of aerosol larger than 0.8  $\mu$  in urban and tropical rainforest locations, *Atmos. Chem. Phys.*,  
391 11(11), 5491–5504, doi:10.5194/acp-11-5491-2011, 2011.
- 392 Górný, R. L.: Filamentous microorganisms and their fragments in indoor air - A review, *Ann.*  
393 *Agric. Environ. Med.*, 11(2), 185–197, doi:10.1007/BF02677055, 2004.
- 394 Hernandez, M., Perring, A. E., McCabe, K., Kok, G., Granger, G. and Baumgardner, D.:  
395 Chamber catalogues of optical and fluorescent signatures distinguish bioaerosol classes,  
396 *Atmos. Meas. Tech.*, 9(7), 3283–3292, doi:10.5194/amt-9-3283-2016, 2016.
- 397 Hill, S. C., Pinnick, R. G., Niles, S., Pan, Y.-L., Holler, S., Chang, R. K., Bottinger, J., Chen, B. T.,  
398 Orr, C.-S. and Feather, G.: Realtime Measurement of Fluorescence Spectra from Single  
399 Airborne Biological Particles, *F. Anal. Chem. Technol.*, 3(4–5), 221–239,  
400 doi:10.1002/(SICI)1520-6521(1999)3:4/5<221::AID-FACT2>3.3.CO;2-Z, 1999.
- 401 Huffman, J. A., Treutlein, B. and Pöschl, U.: Fluorescent biological aerosol particle  
402 concentrations and size distributions measured with an Ultraviolet Aerodynamic Particle  
403 Sizer (UV-APS) in Central Europe, *Atmos. Chem. Phys.*, 10(7), 3215–3233, doi:10.5194/acp-





- 404 10-3215-2010, 2010.
- 405 Kaliszewski, M., Trafny, E. A., Lewandowski, R., Włodarski, M., Bombalska, A., Kopczyński, K.,  
406 Antos-Bielska, M., Szpakowska, M., Młyńczak, J., Mularczyk-Oliwa, M. and Kwaśny, M.: A  
407 new approach to UVAPS data analysis towards detection of biological aerosol, *J. Aerosol Sci.*,  
408 58, 148–157, doi:<https://doi.org/10.1016/j.jaerosci.2013.01.007>, 2013.
- 409 Kaliszewski, M., Włodarski, M., Młyńczak, J., Leśkiewicz, M., Bombalska, A., Mularczyk-Oliwa,  
410 M., Kwaśny, M., Buliński, D. and Kopczyński, K.: A new real-time bio-aerosol fluorescence  
411 detector based on semiconductor CW excitation UV laser, *J. Aerosol Sci.*, 100, 14–25,  
412 doi:[10.1016/j.jaerosci.2016.05.004](https://doi.org/10.1016/j.jaerosci.2016.05.004), 2016.
- 413 Kohlus, R. and Bottlinger, M.: Particle Shape Analysis as an example of knowledge extraction  
414 by neural nets, *Part. Part. Syst. Character.*, 10(5), 275–278, doi:[10.1002/ppsc.19930100511](https://doi.org/10.1002/ppsc.19930100511),  
415 1993.
- 416 Lakowicz, J. R.: Principles of Fluorescence Spectroscopy, Second., Kluwer Academic/Plenum  
417 Publishers., 1999.
- 418 Lee, B. U., Jung, J. H., Yun, S. H., Hwang, G. B. and Bae, G. N.: Application of UVAPS to real-  
419 time detection of inactivation of fungal bioaerosols due to thermal energy, *J. Aerosol Sci.*,  
420 41(7), 694–701, doi:<https://doi.org/10.1016/j.jaerosci.2010.04.003>, 2010.
- 421 Leśkiewicz, M., Kaliszewski, M., Mierczyk, Z. and Włodarski, M.: Comparison of Principal  
422 Component Analysis and Linear Discriminant Analysis applied to classification of excitation-  
423 emission matrices of the selected biological material, *Biul. Wojsk. Akad. Tech.*, 65(1), 15–31,  
424 doi:[10.5604/12345865.1197960](https://doi.org/10.5604/12345865.1197960), 2016.
- 425 Lim, D. V., Simpson, J. M., Kearns, E. A. and Kramer, M. F.: Current and developing  
426 technologies for monitoring agents of bioterrorism and biowarfare, *Clin. Microbiol. Rev.*,  
427 18(4), 583–607, doi:[10.1128/CMR.18.4.583-607.2005](https://doi.org/10.1128/CMR.18.4.583-607.2005), 2005.
- 428 Mauderly, J. L. and Chow, J. C.: Health effects of organic aerosols., 2008.
- 429 Miaskiewicz-Peska, E. and Lebkowska, M.: Comparison of aerosol and bioaerosol collection  
430 on air filters, *Aerobiologia (Bologna)*, 28(2), 185–193, doi:[10.1007/s10453-011-9223-1](https://doi.org/10.1007/s10453-011-9223-1),  
431 2012.
- 432 Michaels, R. A.: Environmental Moisture, Molds, and Asthma—Emerging Fungal Risks in the  
433 Context of Climate Change, *Environ. Claims J.*, 29(3), 171–193,  
434 doi:[10.1080/10406026.2017.1345521](https://doi.org/10.1080/10406026.2017.1345521), 2017.



- 435 Pan, Y. Le, Hill, S. C., Pinnick, R. G., House, J. M., Flagan, R. C. and Chang, R. K.: Dual-  
436 excitation-wavelength fluorescence spectra and elastic scattering for differentiation of single  
437 airborne pollen and fungal particles, *Atmos. Environ.*, 45(8), 1555–1563,  
438 doi:10.1016/j.atmosenv.2010.12.042, 2011.
- 439 Pan, Y. Le, Huang, H. and Chang, R. K.: Clustered and integrated fluorescence spectra from  
440 single atmospheric aerosol particles excited by a 263- and 351-nm laser at New Haven, CT,  
441 and Adelphi, MD, *J. Quant. Spectrosc. Radiat. Transf.*, 113(17), 2213–2221,  
442 doi:10.1016/j.jqsrt.2012.07.028, 2012.
- 443 Pinnick, R. G., Hill, S. C., Pan, Y. Le and Chang, R. K.: Fluorescence spectra of atmospheric  
444 aerosol at Adelphi, Maryland, USA: Measurement and classification of single particles  
445 containing organic carbon, *Atmos. Environ.*, 38(11), 1657–1672,  
446 doi:10.1016/j.atmosenv.2003.11.017, 2004.
- 447 Pöhlker, C., Huffman, J. A. and Pöschl, U.: Autofluorescence of atmospheric bioaerosols:  
448 Spectral fingerprints and taxonomic trends of pollen, *Atmos. Meas. Tech.*, 6(12), 3369–3392,  
449 doi:10.5194/amt-6-3369-2013, 2013.
- 450 Pope III, C. A. and Dockery, D. W.: 2006 Critical Review: Health Effects of Fine Particulate Air  
451 Pollution: Lines That Connect, *J. Air Waste Manag. Assoc.*, 56(6), 709–742,  
452 doi:10.1080/10473289.2006.10464485, 2006.
- 453 Pósfai, M. and Buseck, P. R.: Nature and Climate Effects of Individual Tropospheric Aerosol  
454 Particles, *Annu. Rev. Earth Planet. Sci.*, 38(1), 17–43,  
455 doi:10.1146/annurev.earth.031208.100032, 2010.
- 456 Purnomo, H. D., Hartomo, K. D. and Prasetyo, S. Y. J.: Artificial Neural Network for Monthly  
457 Rainfall Rate Prediction, *IOP Conf. Ser. Mater. Sci. Eng.*, 180(1), 12057, 2017.
- 458 Ruske, S., Topping, D. O., Foot, V. E., Kaye, P. H., Stanley, W. R., Crawford, I., Morse, A. P. and  
459 Gallagher, M. W.: Evaluation of machine learning algorithms for classification of primary  
460 biological aerosol using a new UV-LIF spectrometer, *Atmos. Meas. Tech.*, 10(2), 695–708,  
461 doi:10.5194/amt-10-695-2017, 2017.
- 462 Shiraiwa, M., Selzle, K. and Pöschl, U.: Hazardous components and health effects of  
463 atmospheric aerosol particles: reactive oxygen species, soot, polycyclic aromatic compounds  
464 and allergenic proteins, *Free Radic. Res.*, 46(8), 927–939,  
465 doi:10.3109/10715762.2012.663084, 2012.
- 466 Taketani, F., Kanaya, Y., Nakamura, T., Koizumi, K., Moteki, N. and Takegawa, N.:  
467 Measurement of fluorescence spectra from atmospheric single submicron particle using



468 laser-induced fluorescence technique, *J. Aerosol Sci.*, 58, 1–8,  
469 doi:<https://doi.org/10.1016/j.jaerosci.2012.12.002>, 2013.

470 Trafny, E. A., Lewandowski, R., Stępińska, M. and Kaliszewski, M.: Biological threat detection  
471 in the air and on the surface: How to define the risk, *Arch. Immunol. Ther. Exp. (Warsz.)*,  
472 62(4), 253–261, doi:[10.1007/s00005-014-0296-8](https://doi.org/10.1007/s00005-014-0296-8), 2014.

473

474